Journal of Photochemistry and Photobiology A: Chemistry 216 (2010) 15–23

Contents lists available at ScienceDirect

Journal of Photochemistry and Photobiology A: Chemistry

journal homepage: www.elsevier.com/locate/jphotochem

# *Meso-meso* linked diporphyrin functionalized single-walled carbon nanotubes

Lin He [a], Yi-Zhou Zhu [a], Jian-Yu Zheng [a,*], Yan-Feng Ma [b], Yong-Sheng Chen [b]

[a] State Key Laboratory and Institute of Elemento-Organic Chemistry, Nankai University, 94 Weijin Road, Nankai District, Tianjin 300071, China
[b] Center for Nanoscale Science and Technology and Key Laboratory for Functional Polymer Materials, Institute of Polymer Chemistry, College of Chemistry, Nankai University, Tianjin 300071, China

ARTICLE INFO

*Article history:*
Received 9 April 2010
Received in revised form 17 August 2010
Accepted 3 September 2010
Available online 15 September 2010

*Key words:*
*Meso-meso* linked diporphyrin
Single-walled carbon nanotube
Charge separate
Photoinduced electron transfer

ABSTRACT

*Meso-meso* linked diporphyrins ($[H_2Por]_2$) covalently functionalized soluble single-walled carbon nanotubes ($[H_2Por]_2$-SWNTs) have been successfully prepared. As a light-harvesting chromophore, *meso-meso* linked diporphyrins have been incorporated into a photosynthetic electron-transfer model with SWNTs as an electron-acceptor. The steady emission characteristics revealed the existence of the effective energy and electron transfer between the excited porphyrin moiety and SWNTs, and the electron transfer process was confirmed by electrochemical study. The charge separation quenching process was supported by the results of time-resolved transient absorption spectra, and the lifetime of charge-separation state was observed to be 145 ns, which was 2.5 times of that of monoporphyrin modified SWNTs (TPP-SWNTs).



## 1. Introduction

Carbon nanotubes are actively being investigated for producing photoelectronic and photovoltaic devices [1–6] because of their high delocalized, extended π-electron system [7,8]. Especially, most single-walled carbon nanotubes (SWNTs) have the diameter of approximately 1 nm, which results in a higher aspect ratio and a greater curvature of the sidewall. That further alters the extent of orbital overlap and the electronic density [9], and makes them be natural electron acceptor [10–12]. SWNTs have thus been widely used combining with light absorbing antenna chromophores to construct photovoltaic devices [1,13–17]. Porphyrins are known chromophores, which play an important role in natural photosynthetic system due to their unique photophysical and electrochemical properties [18–20]. In the past decades, porphyrins have been broadly applied in the research of artificial photosynthetic mimic systems [21–29]. In view of the distinct advantages of porphyrin and SWNTs, a number of SWNTs–porphyrin nanohybrids, constructed by π–π and Van der Waals [30–34], polymer wrapping [35,36], electrostatic interaction [37–40] or covalent bond [41–46], have been built to be photoelectron transfer models.

As mentioned above, porphyrins functionalized SWNTs have attracted extensive attention as excellent candidates for nanoscale photovoltaic devices. Some covalently linked porphyrin-functionalized SWNTs [42–44] have previously been synthesized in our group for the research of energy and electron transfer. We found an 86% reduction of fluorescence quantum yield in the nanohybrid employing amide linkage between SWNTs and porphyrin [43], while more than 97% reduction with a direct linkage mode [42]. Obviously, the direct linkage mode facilitated the effective energy and electron transfer between the excited porphyrin moiety and SWNTs. We report here the preparation of the *meso-meso* linked diporphyrin functionalized SWNTs with a direct linkage. The replacement of monoporphyrin with *meso-meso* linked diporphyrin can result in a broader absorption, which attributes to the exciton coupling of the porphyrin subunits [47–54]. Furthermore, *meso-meso* linked diporphyrin has prolonged charge-separation (CS) lifetime of porphyrin–acceptor system compared with monoporphyrin [50]. Therefore, *meso-meso* linked diporphyrin functionalized SWNTs ($[H_2Por]_2$-SWNTs) (Scheme 1) is rationally expected to be an improved photon-to-electron conversion system.

## 2. Results and discussion

### 2.1. Synthesis and characterization

The *meso-meso* linked diporphyrin functionalized SWNTs ($[H_2Por]_2$-SWNTs) was prepared by the reaction of octadecylamine modified SWNTs (ODA-SWNTs) with the corresponding diporphyrin diazonium compound generated from diporphyrin amino compound *in situ* (Scheme 2) [42,55]. The diporphyrin was obtained *via* a Suzuki-coupling reaction (Scheme 3) [56].

The Raman spectrum of $[H_2Por]_2$-SWNTs was significantly different from that of ODA-SWNTs (Fig. 1). Compared to ODA-SWNTs, more structure information could be found except for the tangential mode at ~1590 $cm^{-1}$ (G-band) and the disorder

* Corresponding author. Tel.: +86 22 23505572; fax: +86 22 23505572.
*E-mail address:* jyzheng@nankai.edu.cn (J.-Y. Zheng).

1010-6030/$ – see front matter © 2010 Elsevier B.V. All rights reserved.
doi:10.1016/j.jphotochem.2010.09.001

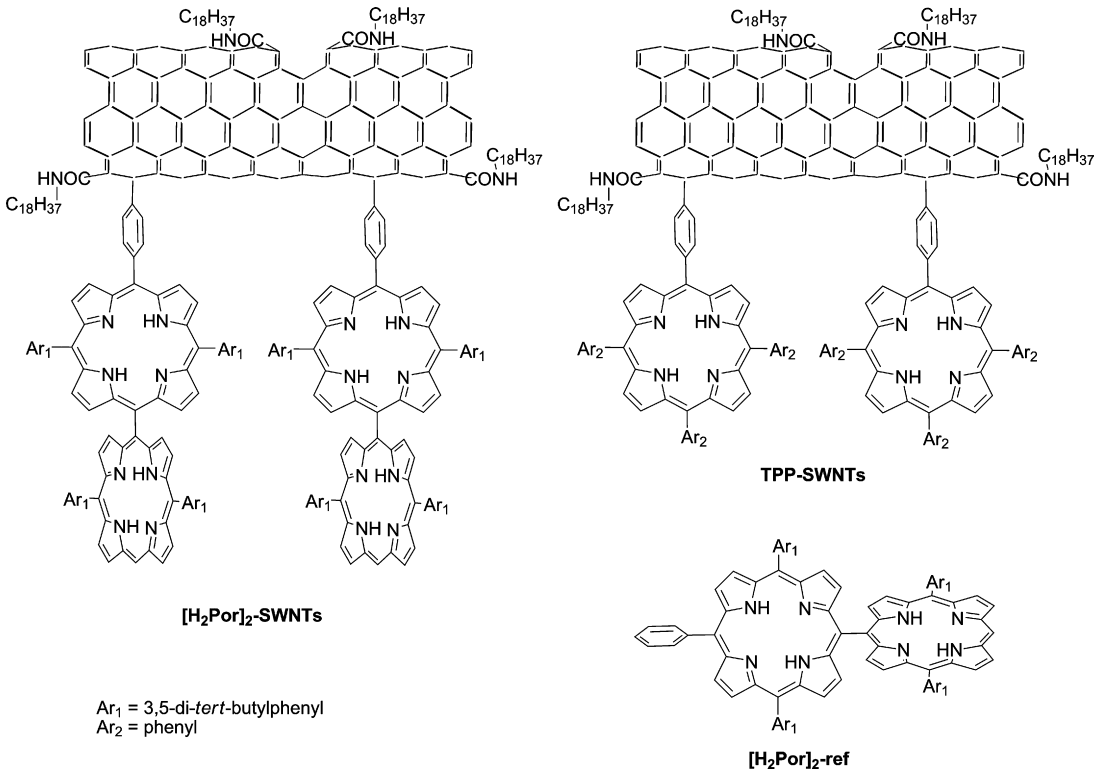


**Scheme 1.** Structures of porphyrin–SWNTs dyads and reference compounds.

mode at ~1350 $cm^{-1}$ (D-band). The additional peaks at 819, 1002, 1082, 1234, 1454, 1494, and 1553 $cm^{-1}$ could be assigned to the covalently attached porphyrin moiety [57]. Meanwhile, the FTIR spectrum of $[H_2Por]_2$-SWNTs (see ESI, Fig. S1) exhibited the characteristic porphyrin absorptions at 3306, 3060, 1537, 1419, 1022, 792, and 684 $cm^{-1}$. The absorption bands at 3306 and 3060 $cm^{-1}$ could be separately assigned to the stretching vibration of the pyrrole N–H and aromatic C–H of the diporphyrins. The bands at 3343, 2921, 2850, and 1646 $cm^{-1}$ derived from the moieties of octadecylamine. These Raman and IR data indicate a successful functionalization of SWNTs with diporphyrins.

Consisting with Raman and FTIR results, the transmission electron microscopy (TEM) images showed more direct evidence for the successful modification. Fig. 2 shows the typical surface morphology of SWNTs before and after porphyrin functionalization. The sidewall of the SWNTs was significantly roughened by the coverage of soft materials, indicating the presence of porphyrin attached to the SWNTs surface. The content of porphyrin moiety

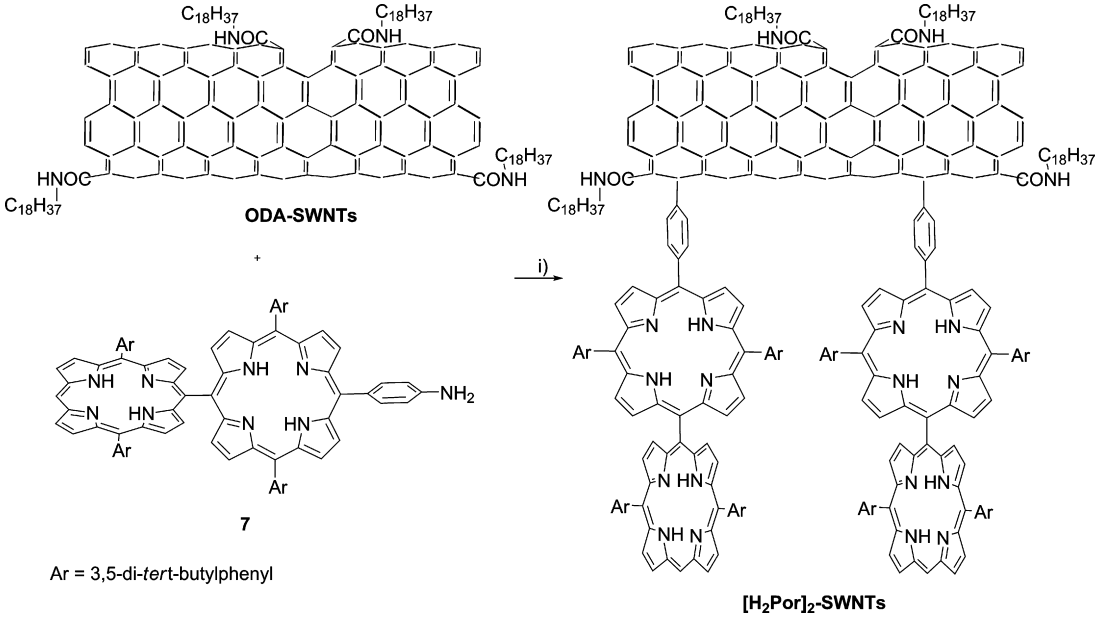


**Scheme 2.** Preparation of $[H_2Por]_2$-SWNTs: (i) 70 °C, isoamyl nitrite, ODCB.

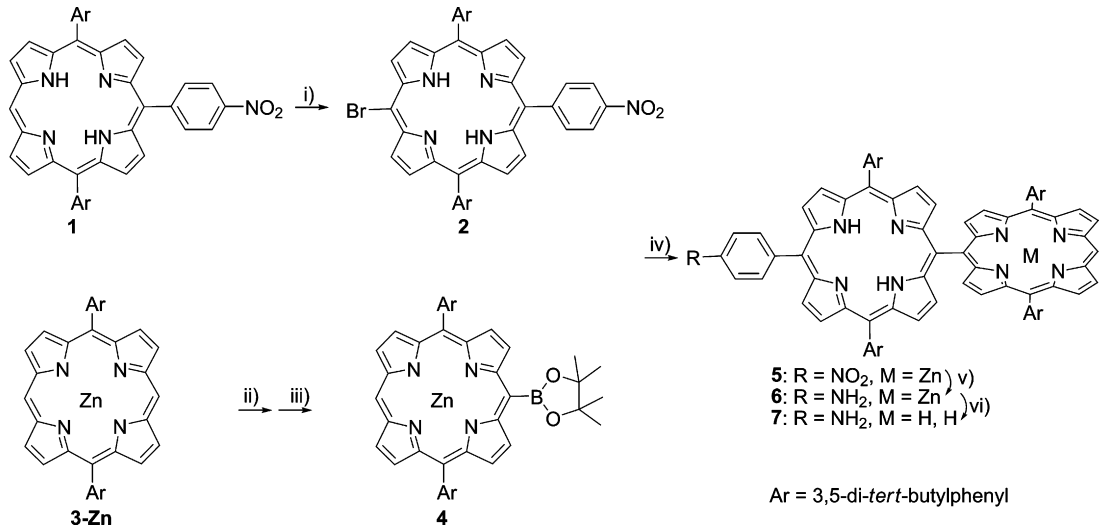


**Scheme 3.** Preparation of *meso-meso* linked diporphyrin: (i) NBS, $CHCl_3$/MeOH; 91%; (ii) NBS, $CH_2Cl_2$/MeOH; (iii) 90 °C, 4,4,5,5-tetramethyl-1,3,2-dioxaborolane, $Pd(PPh_3)_2Cl_2$, triethylamine, 1,2-dichloroethane; 40% (two steps); (iv) 80 °C, $Pd(PPh_3)_4$, $Cs_2CO_3$, DMF/toluene; 68%; (v) 5% Pd/C, $NaBH_4$, $CH_2Cl_2$/MeOH; (vi) $CF_3COOH$, $CHCl_3$; 67% (two steps).

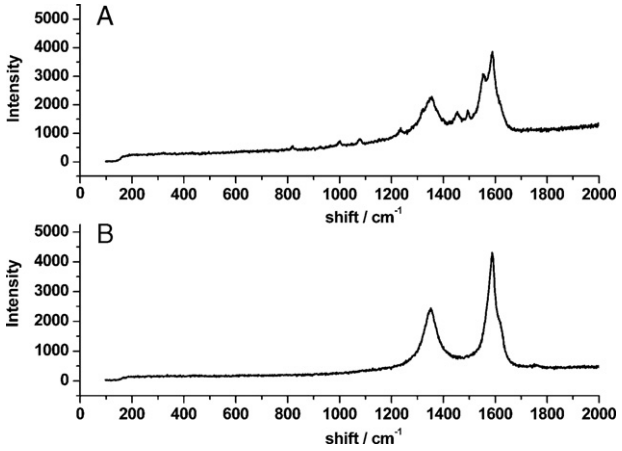


**Fig. 1.** Raman spectra of $[H_2Por]_2$-SWNTs (A) and ODA-SWNTs (B).

in $[H_2Por]_2$-SWNTs nanohybrid could be estimated in the light of the elemental composition of ODA-SWNTs and $[H_2Por]_2$-SWNTs (Table 1), determined by X-ray photoelectron spectroscopy (XPS). The content of diporphyin unit in $[H_2Por]_2$-SWNTs, one diporphyrin unit per ~600 C atoms, is similar to the content of monoporphyrin unit in TPP-SWNTs nanohybrid.

### 2.2. Steady state absorption spectroscopy

The steady state absorption spectrum of $[H_2Por]_2$-SWNTs in ODCB (Fig. 3) showed two split Soret bands (423 and 459 nm) and four Q-bands (530, 569, 601, and 662 nm). There was one more Soret band than the absorption spectrum of monoporphyrin functionalized SWNTs (TPP-SWNTs) (Fig. 3). Compared to $[H_2Por]_2$-ref, there were 4–7 nm red-shift for both Soret bands and Q-bands, and simultaneously with notable broadening of the Soret bands. Those reflect that the covalent bonding to SWNTs causes a change of the electronic states of diporphyrin, and there is notable electronic communication between SWNTs and diporphyrin in the ground state [58]. The absorption spectra of $[H_2Por]_2$-SWNTs with different concentrations were measured, and the absorption values at 419 and 459 nm were plotted against concentrations to get a standard curve (in mg $L^{-1}$, Fig. 4). On the basis of Beer's law, the effective extinction coefficient of $[H_2Por]_2$-SWNTs was determined to be 0.03 L $mg^{-1}$ $cm^{-1}$ in accordance with the slope of the linear least-squares fit. The absorption values of $[H_2Por]_2$-SWNTs at different wavelengths were well in line with the correlative concentrations, proving that the solution was homogeneous. The solubility could be calculated to be 355 mg $L^{-1}$ according to the Beer's law, and the solution in ODCB was stable for several months (Fig. 5). The good solubility indicates the exfoliating of nanotube bundles.

**Table 1**
XPS elemental composition for *o*-SWNTs, ODA-SWNTs, TPP-SWNTs and $[H_2Por]_2$-SWNTs.

| Sample | XPS elemental composition[a] | | |
|---|---|---|---|
| | C1s | N1s | O1s |
| *o*-SWNTs[b] | 83.41 | 0.00 | 16.59 |
| ODA-SWNTs | 86.50 | 1.18 | 12.32 |
| TPP-SWNTs | 84.72 | 1.49 | 13.79 |
| $[H_2Por]_2$-SWNTs | 92.01 | 1.86 | 6.13 |

[a] The elemental composition was measured as atomic conc.
[b] *o*-SWNTs is the abbreviation of oxide SWNTs.

### 2.3. Steady state emission spectroscopy

The excited state interactions between SWNTs and diporphyrins were explored by steady state fluorescence spectra of $[H_2Por]_2$-ref and $[H_2Por]_2$-SWNTs. $[H_2Por]_2$-SWNTs exhibited complete fluorescence quenching (100%, Fig. 6), upon excitation of the porphyrin moiety at 419 and 453 nm. Even when the absorption of SWNTs was subtracted from the absorbance of $[H_2Por]_2$-SWNTs, the fluorescence also exhibited almost complete quenching (99%) (see ESI, Fig. S2). The complete luminescence quenching indicates that there is a strong interaction between the excited diporphyrin and SWNTs [42]. Possible pathways for the deactivation of excited porphyrins may be attributed to two competitive processes, energy transfer (ET) and photoinduced electron transfer (PET). The emission band of $[H_2Por]_2$ (between 620 and 800 nm) overlaps with the absorption band of SWNTs, which enables singlet–singlet energy transfer from diporphyrin to SWNTs [59]. Nevertheless, the fluorescence quantum yield of $[H_2Por]_2$-SWNTs significantly decreased against increasing solvent polarity (Table 2), which indicates that the quenching process in $[H_2Por]_2$-SWNTs nanohybrid is mainly dominated by the excited state electron transfer, because the energy transfer commonly does not depend on solvent polarity while the electron transfer tends to be sensitive to medium effects [42,60,61].

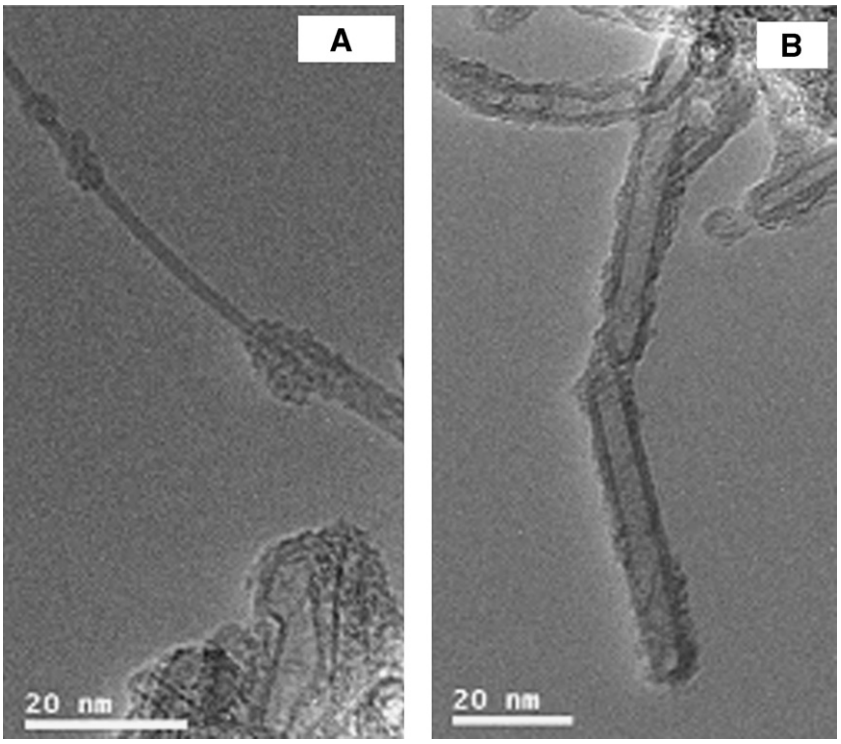


**Fig. 2.** TEM images of ODA-SWNTs (A) and $[H_2Por]_2$-SWNTs (B).

### 2.4. Electrochemistry analysis

Electrochemical studies with cyclic voltammetry (CV) were performed to understand the overall redox behavior of $[H_2Por]_2$-SWNTs, evaluate the electronic properties of the nanohybrid, and also visualize the existence of any electronic interaction between diporphyrins and SWNTs. The CV of $[H_2Por]_2$-ref showed two oxidation and one reduction processes (see ESI, Fig. S3). The first reduction peak was observed at −1.57 V versus $Ag/Ag^+$, and the two oxidation peaks were seen at +0.66 and +0.90 V, respectively. The redox properties of the mixture of ODA-SWNTs and $[H_2Por]_2$-ref (ODA-SWNTs + $[H_2Por]_2$-ref) did not show any significant variations compared to $[H_2Por]_2$-ref (Table 3). However, obvious variations were found in the oxidation and reduction potentials of $[H_2Por]_2$-SWNTs. The first oxidation peek was observed at +0.32 V with a cathodic shift of ~340 mV, which can be attributed to the fast electron transfer in $[H_2Por]_2$-SWNTs as a result of limited access of the SWNTs bound redox probes to the electrode surface [63]. One more reduction peek at −0.49 V appeared in $[H_2Por]_2$-SWNTs, which corresponded to the reduction potential of SWNTs [63]. The change of redox properties of porphyrin moiety indicates the diporphyrin becomes easier to be oxidized. The free-energy changes for charge separation ($\Delta G_{cs}$) was calculated according to the Rehm–Weller method (Eq. (1)), by employing the first oxidation potential of diporphyrin ($E^1_{ox}$), the first reduction potential of SWNTs ($E^1_{red}$), and the singlet excitation energy of $[H_2Por]_2$-ref ($\Delta E_{0-0}$) [64]:

$$\Delta G_{CS} = E^1_{ox} - E^1_{red} - \Delta E_{0-0} \quad (1)$$

Herein, $\Delta E_{0-0}$ (1.81 eV) was determined by the 0–0* absorption. The $\Delta G_{CS}$ value for generating the radical ion pair $[H_2Por]_2^{\bullet+}$-$SWNTs^{\bullet-}$ was found to be −1.00 eV, which indicates the possibility of photoinduced charge separation in the nanohybrid. It should be noted that the Coulombic terms in the present donor–acceptor systems are negligible, especially in solvents with moderate or high polarity, because of the relatively long edge-to-edge distance (*R*ee > 11 Å) employed [65–70].

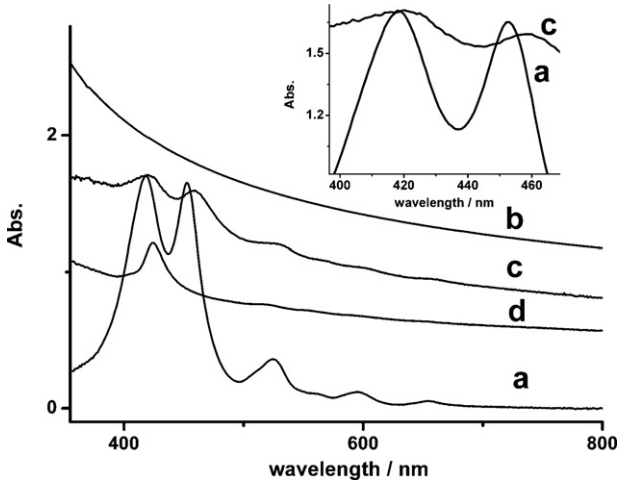


**Fig. 3.** UV–vis spectra of $[H_2Por]_2$-ref (a), ODA-SWNTs (b), $[H_2Por]_2$-SWNTs (c), and TPP-SWNTs (d) in ODCB. The inset showed the Soret-band region in more details.

### 2.5. Transient absorption spectroscopy

Time-resolved transient absorption spectrum, following nanosecond laser pulses, was employed to examine the photodynamics of $[H_2Por]_2$-SWNTs nanohybrid. It provided evidence for charge separation and allowed us to estimate the charge recombination rates, $k_{CR}$. Fig. 7 shows a broad absorption band between 460 and 680 nm, which is the typical absorption of radical cation $[H_2Por]_2^{\bullet+}$ of $[H_2Por]_2$-SWNTs nanohybrid [50]. Meanwhile, a net decrease was observed around 420, 460, 570, 600, and 650 nm due to $^1[H_2Por]_2^*$, which are dominated by the ground state absorption of diporphyrin. Therefore, the photoinduced electron transfer process involved from $^1[H_2Por]_2^*$ to SWNTs and, in turn,

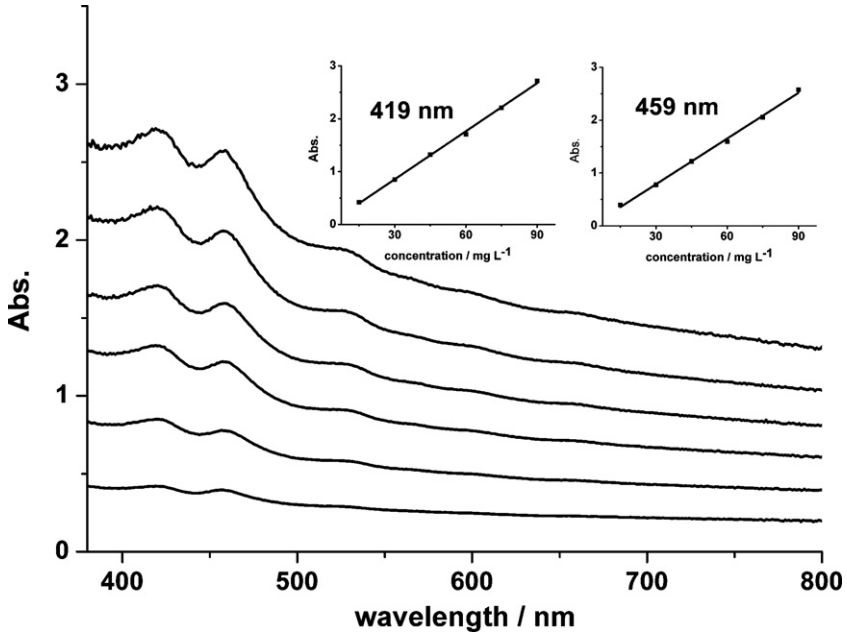


**Fig. 4.** Absorption spectra of $[H_2Por]_2$–SWNTs in ODCB (concentrations are 15, 30, 45, 60, 75, 90 mg $L^{-1}$, respectively). Shown in the inset are the plots of absorbency at 419 and 459 nm versus concentration. The straight lines are linear least-square fit to the data.

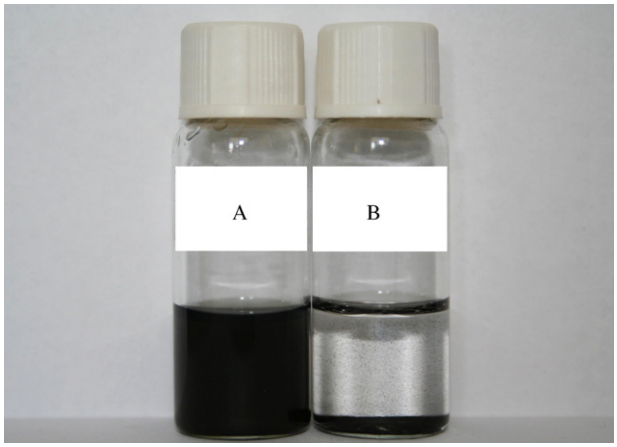


**Fig. 5.** The state of $[H_2Por]_2$-SWNTs (A) and ODA-SWNTs (B) solutions in ODCB after two months.

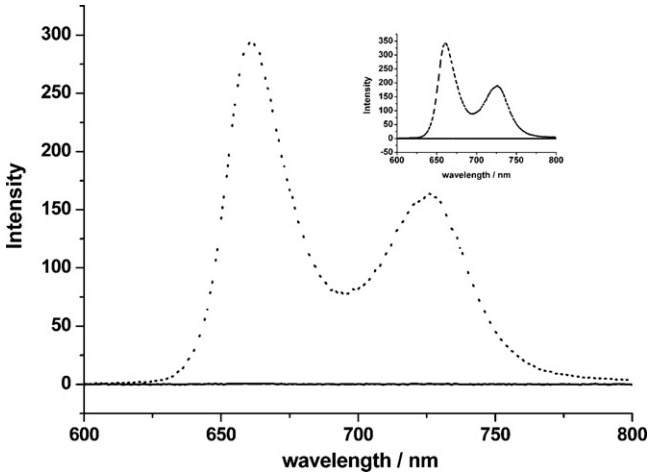


**Fig. 6.** Fluorescence spectra of $[H_2Por]_2$-ref (dotted) and $[H_2Por]_2$-SWNTs (solid) in ODCB excited at 419 and 453 nm (the inset), respectively.

**Table 2**
Relative fluorescence quantum yields of $[H_2Por]_2$-SWNTs in solvents of different polarity.

| Solvent | Dielectric constant[a] | Relative $\Phi_f$[b] |
|---|---|---|
| Toluene | 2.38 | 1.0 |
| THF | 7.58 | 0.48 |
| ODCB | 9.93 | 0.28 |

Solutions were deoxygenated by purging with $N_2$ before quantum yields were determined.

[a] From Ref. [62].
[b] Measured at 298 K.

created the $[H_2Por]_2^{\bullet+}$-SWNTs$^{\bullet-}$ state, as shown in Scheme 4. The time-resolved transient absorption spectrum confirmed the existence of electron transfer. The lifetime of the charge separation state ($[H_2Por]_2^{\bullet+}$-SWNTs$^{\bullet-}$) was evaluated to be 145 ns from transient absorption kinetics measurement at 620 nm (Fig. 7), and the $k_{CR}$ was calculated to be $6.9 \times 10^6\ S^{-1}$. However, the CS lifetime of TPP-SWNTs and the corresponding $k_{CR}$ were determined to be 57 ns and $1.8 \times 10^7\ S^{-1}$ separately. The significant decrease of charge recombination rate, compared to TPP-SWNTs nanohybrid, makes it more feasible to build photovoltaic device.

## 3. Experimental

### 3.1. Instruments and measurements

UV–vis spectra were recorded on a VARIAN Cary 300 spectrophotometer using a quartz cell with a path length of 10 mm. Fluorescence spectra were obtained with a Cary Eclipse spectrometer. FTIR spectra were obtained with a BRUKER TENSOR 27

**Table 3**
Redox potentials (versus $Ag/Ag^+$) of $[H_2Por]_2$-ref, SWNTs + $[H_2Por]_2$-ref, and $[H_2Por]_2$-SWNTs.

| Sample | $E^2_{ox}$/V | $E^1_{ox}$/V | $E_{red}$/V |
|---|---|---|---|
| $[H_2Por]_2$-ref | 0.90 | 0.66 | −1.57 |
| SWNTs + $[H_2Por]_2$-ref | 0.91 | 0.66 | −1.58 |
| $[H_2Por]_2$-SWNTs | | 0.32 | −0.49 |

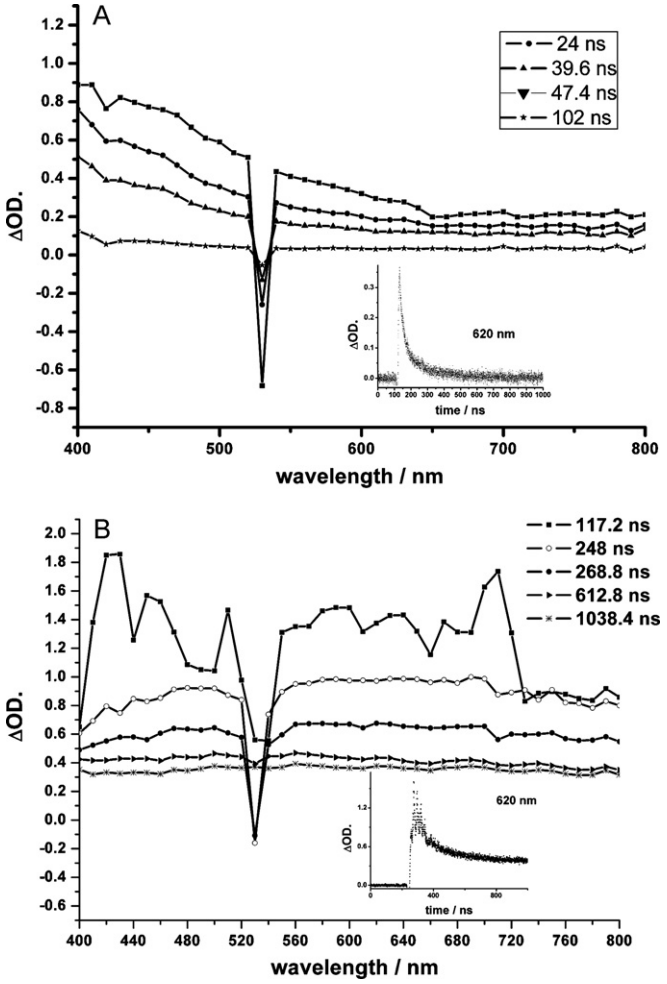


**Fig. 7.** Nanosecond transient absorption spectra of TPP-SWNTs (A) and $[H_2Por]_2$-SWNTs (B) observed by laser irradiation at 532 nm in THF. The insets showed the time profiles of absorbance at 620 nm.

instrument. All IR samples were prepared as films on pellets of spectroscopic grade KBr with solution in $CH_2Cl_2$. Raman spectra were measured by a Reinishaw *via* Raman microscope at room temperature with the 514.5 nm line of an Ar ion laser as an excitation source. $^1$H NMR and $^{13}$C NMR spectra were recorded on Bruker (300 MHz or 400 MHz) or VARIAN (400 MHz) spectrometer using TMS as the internal standard. Mass spectra were recorded on a FTICR-MS, using ESI ionization method. Separations of SWNTs from the impurities were performed with a centrifuge (Eppendorf 5810R), and filtration was performed through a nylon membrane (Whatman International Ltd., England/MAGNA, 0.22/0.1 μm). Ultrasonication was done in a KQ-400KDE (400 W, 40 kHz, Kunshan Sonicator Instrument Co. Inc.) bath sonicator. X-ray photoelectron spectroscopy (XPS) were recorded using a Kratos Axis Ultra DLD spectrometer employing a monochromated Al-Ka X-ray source ($h\nu$ = 1486.6 eV), hybrid (magnetic/electrostatic) optics and a multi-channel plate and delay line detector (DLD). All XPS spectra were recorded using an aperture slot of 300 μm × 700 μm, survey spectra were recorded with a pass energy of 160 eV, and high resolution spectra with a pass energy of 40 eV. Transmission electron microscope (TEM) images were obtained on a FEI TECNAI-20 instrument operated at 100 kV. Sample preparation involved sonicating materials in THF for 30 min and dropping the resulting suspension onto carbon-coated copper grids. Redox potentials were measured by cyclic voltammetry on a BAS electrochemical analyzer model 660. All experiments were carried out using a conventional three-electrode system employing a glassy carbon electrode as the working electrode, $Ag/Ag^+$ electrode as the reference electrode, and a Pt wire as the counter electrode. The redox potentials were measured by cyclic voltammetry in ODCB, using 0.04 M *n*-$Bu_4NPF_6$ as supporting electrolyte with a scan rate of 100 mV s$^{-1}$. Nanosecond transient absorption measurements were carried out using the third (532 nm) harmonic of *Q*-switched Nd:YAG laser (Continuum Surelite I, fwhm 7 ns) as excitation source and a Germanium Photodiode (Edinburgh Lp900) was used as a detector. All of the sample were dissolved in THF, and deaerated with Ar bubbling for 30 min at room temperature.

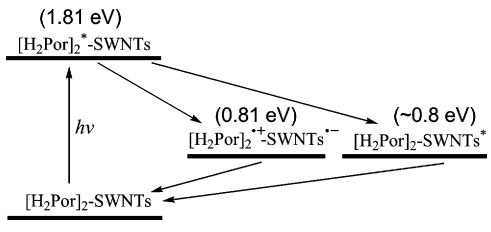


**Scheme 4.** Photo-reaction route of $[H_2Por]_2$-SWNTs in THF (the energy of excited SWNT is from Ref. [71]).

### 3.2. Materials

The pristine carbon nanotube was purchased from Shenzhen Nanotech Port Co., individual tubes of SWNTs have a diameter range of <2 nm. All of solvents were purified according to standard methods. Acetonitrile, *o*-dichlorobenzene (ODCB), chloroform, dichloromethane, 1,2-dichloroethane and N,N-dimethylformamide (DMF) were distilled from calcium hydride before use. THF and toluene were dried and distilled from sodium. All other chemicals (AR) obtained from commercial sources were used without any further purification.

### 3.3. Preparation

5,15-Di(3,5-di-*tert*-butyl)phenylporphinatozinc **3-Zn**, 5,15-di(3,5-di-*tert*-butyl)phenyl-10-(4,4,5,5-tetramethyl-1,3,2-dioxaborolan-2-yl)porphinatozinc (**4**), and 5-(*p*-aminophenyl)-10,15,20-triphenylporphyrin (TPP-$NH_2$), were prepared according to the literature [72,73].

#### 3.3.1. Synthesis of 5,15-di(3,5-di-tert-butylphenyl)-10-(4-nitrophenyl)porphyrin (*1*)

To a solution of 4-nitrophenyldipyrromethane (1.06 g, 3.2 mmol) and 3,5-di-*tert*-butylbenzaldehyde (1.21 g, 5.6 mmol) in 950 mL dry dichloromethane pumped with $N_2$ for 15 min, TFA (0.73 g, 6.4 mmol) was added, then dipyrromethane (0.41 g, 2.8 mmol) in 75 mL dry dichloromethane was added dropwise for 30 min. The mixture was stirred at room temperature for 1 h, then treated with DDQ (1.41 g, 6.2 mmol) and stirred for another 2 h. Removal of solvent and chromatography afforded a purple solid (185 mg, 8%). $^1$H NMR ($CDCl_3$): $\delta$ 10.28 (s, 1H), 9.38 (d, $J$ = 4.5 Hz, 2H), 9.09 (d, $J$ = 4.5 Hz, 2H), 9.00 (d, $J$ = 4.5 Hz, 2H), 8.76 (d, $J$ = 4.5 Hz, 2H), 8.64 (d, $J$ = 8.7 Hz, 2H), 8.41 (d, $J$ = 8.4 Hz, 2H), 8.11 (d, $J$ = 1.5 Hz, 4H), 7.83 (t, $J$ = 1.5 Hz, 2H), 1.55 (s, 36H), −2.96 ppm (s, 2H).

#### 3.3.2. Synthesis of 5-bromo-15-(4-nitrophenyl)-10,20-di(3,5-di-tert-butylphenyl)-porphyrin *2*

NBS (5 mg, 0.028 mmol) was added to a stirred solution of **1** (21 mg, 0.026 mmol) in 50 mL $CHCl_3$/MeOH (9:1) at room temperature. After 10 min, the reaction was quenched with acetone (2 mL). Removal of solvent and the residue was crystalled with $CHCl_3$/MeOH to afford the product as a purple solid (21 mg, 91%).

$^1$H NMR ($CDCl_3$): $\delta$ 9.70 (d, $J$ = 4.8 Hz, 2H), 8.96 (d, $J$ = 4.8 Hz, 2H), 8.88 (d, $J$ = 4.8 Hz, 2H), 8.69 (d, $J$ = 4.8 Hz, 2H), 8.63 (d, $J$ = 8.4 Hz, 2H), 8.37 (d, $J$ = 8.4 Hz, 2H), 8.05 (d, $J$ = 1.6 Hz, 4H), 7.83 (t, $J$ = 1.6 Hz, 2H) 1.54 (s, 36H), −2.72 ppm (s, 2H).

*3.3.3. Synthesis of $Zn^{II}$-free base hybrid diporphyrin **5***

Bromoporphyrin **2** (119 mg, 0.134 mmol), porphyrin boronate **4** (117.5 mg, 0.134 mmol), $Cs_2CO_3$ (65.6 mg, 0.201 mmol), and $Pd(PPh_3)_4$ (15.5 mg, 0.0134 mmol) were dissolved in a mixture of dry DMF (9 mL) and dry toluene (18 mL). The solution was deoxygenated *via* three freeze–pump–thaw degassing cycles and the resulting mixture was heated at 80 °C for 12 h under Ar. The mixture was extracted with $CH_2Cl_2$, and the organic layer was dried with anhydrous $Na_2SO_4$. Removal of solvent and chromatography afforded a purple solid (142 mg, 68%). $^1$H NMR ($CDCl_3$): $\delta$ 10.41 (s, 1H), 9.51 (d, $J$ = 4.8 Hz, 2H), 9.20 (d, $J$ = 4.8 Hz, 2H), 8.97 (d, $J$ = 4.8 Hz, 2H), 8.81 (d, $J$ = 4.8 Hz, 2H), 8.79 (d, $J$ = 4.8 Hz, 2H), 8.69 (d, $J$ = 8.4 Hz, 2H), 8.60 (d, $J$ = 4.8 Hz, 2H), 8.50 (d, $J$ = 8.4 Hz, 2H), 8.19 (d, $J$ = 4.8 Hz, 2H), 8.11 (d, $J$ = 1.6 Hz, 4H), 8.06 (d, $J$ = 1.6 Hz, 4H), 8.03 (d, $J$ = 4.8 Hz, 2H), 7.72 (t, $J$ = 1.6 Hz, 2H), 7.70 (t, $J$ = 1.6 Hz, 2H), 1.45 (d, $J$ = −13.2 Hz, 72H), −2.15 ppm (s, 2H); ESI-MS $m/z$: 1554.83 ($[M+H]^+$); calcd for $C_{102}H_{108}N_9O_2Zn$ 1554.79.

*3.3.4. Synthesis of meso-meso linked diporphyrin **7***

$Zn^{II}$-free base hybrid diporphyrin **5** (142 mg, 0.091 mmol) was dissolved in $CH_2Cl_2$ (13 mL) and methanol (9 mL), to which 5% Pd/C (54 mg) was added. Then, $NaBH_4$ (47 mg, 1.175 mmol) was added to the solution by portions, and the resulting reaction mixture was stirred for 2 min at room temperature. Pd/C was filtered off and the filtrate was washed with water and the organic layer was dried over anhydrous $Na_2SO_4$. The desiccant was filtered off and the filtrate was treated with TFA at room temperature for an hour. The mixture was washed with saturation $Na_2CO_3$, and the organic layer was dried with anhydrous $Na_2SO_4$. The solvent was removed by a rotary evaporator and the residue was separated by silica gel chromatography with $CH_2Cl_2$ to give purple solid **7** (90 mg, 68%). $^1$H NMR ($CDCl_3$): $\delta$ 10.37 (s, 1H), 9.45 (d, $J$ = 4.8 Hz, 2H), 9.13 (d, $J$ = 4.8 Hz, 2H), 9.04 (d, $J$ = 4.8 Hz, 2H), 8.94 (d, $J$ = 4.8 Hz, 2H), 8.70 (d, $J$ = 4.8 Hz, 2H), 8.62 (d, $J$ = 4.8 Hz, 2H), 8.12 (m, 12H), 8.05 (d, $J$ = 4.8 Hz, 2H), 7.74 (t, $J$ = 1.6 Hz, 2H), 7.71 (t, $J$ = 1.6 Hz, 2H), 7.11 (d, $J$ = 8.4 Hz, 2H), 4.05 (s, 2H), 1.47 (d, $J$ = −10.8 Hz, 72H), −2.09 (s, 2H), −2.32 ppm (s, 2H); $^{13}$C NMR: $\delta$ 149.08, 148.86, 146.25, 141.287, 140.81, 135.82, 132.95, 130.09, 130.02, 129.95, 129.85, 122.47, 122.08, 121.67, 121.31, 121.22, 118.39, 117.87, 113.71, 31.97 ppm; ESI-MS $m/z$: 1462.9027 ($[M+H]^+$); calcd for $C_{102}H_{112}N_9$ 1462.9035.

*3.3.5. Synthesis of porphyrin–SWNTs nanohybrids TPP-SWNTs*

ODA-SWNTs (6.0 mg) was sonicated for 15 min in ODCB (7.5 mL). To this suspension, TPP-$NH_2$ (10 mg, 0.016 mmol) in acetonitrile (2.0 mL) was added. Bubbled with nitrogen for 15 min, isoamyl nitrite (5 μL, 0.037 mmol) was quickly added and the suspension was stirred in the dark at 70 °C under nitrogen for 48 h. During the period, another 50 mg (0.080 mmol) TPP-$NH_2$ and 25 μL (0.19 mmol) isoamyl nitrite were added in 5 portions (total 5× 10 mg TPP-$NH_2$ and 5× 5 μL isoamyl nitrite) to ensure a high degree of functionalization. The suspension was diluted with 10 mL DMF, filtered over a nylon membrane (0.1 μm), and washed with DMF repetitively. The filtered product was sonicated in DMF and filtered repeatedly. Ultimately, the product was washed with $CH_2Cl_2$ and dried in vacuum at 80 °C for 10 h to give TPP-SWNTs (5.8 mg).

*3.3.6. Synthesis of porphyrin–SWNTs nanohybrids $[H_2Por]_2$-SWNTs*

ODA-SWNTs (5.8 mg) was sonicated for 15 min in ODCB (7.5 mL). To this suspension, *meso-meso* linked diporphyrin **7** (18 mg, 0.012 mmol) in acetonitrile (2.0 mL) was added. Bubbled with nitrogen for 15 min, isoamyl nitrite (5 μL, 0.037 mmol) was quickly added and the suspension was stirred in the dark at 70 °C for 48 h. During the period, another 90 mg (0.060 mmol) **7** and 25 μL (0.19 mmol) isoamyl nitrite were added in 5 portions (total 5× 18 mg **7** and 5× 5 μL isoamyl nitrite) to ensure a high degree of functionalization. The suspension was diluted with 10 mL DMF, filtered over a nylon membrane (0.1 μm), and washed repetitively with DMF. The filtered product was sonicated in DMF and filtered repeatedly. Ultimately, the product was washed with $CH_2Cl_2$ and dried in vacuum at 80 °C for 10 h to give $[H_2Por]_2$-SWNTs (6.1 mg).

## 4. Conclusion

In conclusion, we have prepared covalently linked $[H_2Por]_2$-SWNTs nanohybrid for the first time, where *meso-meso* linked diporphyrin is successfully incorporated into a charge separation unit as a photosynthetic electron-transfer model. The nanohybrid reveals photoinduced electron-transfer from the diporphyrin excited singlet state to the SWNTs, which resulted in the generation of $[H_2Por]_2^{\bullet+}$-SWNTs$^{\bullet-}$ radical ion pair with 145 ns lifetime. It should be emphasized here that the CS lifetime of the nanohybrid has been prolonged substantially by replacing monoporphyrin with diporphyrin. The present results demonstrate that *meso-meso* linked diporphyrin is an outstanding electron donor to build SWNTs involving light-energy conversion and photovoltaic devices.

## Supplementary data

FTIR spectra, absorption and emission spectra and cyclic voltammograms of the nanohybrid and reference compounds. The preparation of the reference compound $[H_2Por]_2$-ref.

## Acknowledgements

We would like to thank Associate Professor Yuping Liu for her work on XPS measurement. This work is supported by the 973 Program (2006CB932900), NSFC (Nos. 20721062 and 20802038) and Tianjin Natural Science Foundation (07QTPTJC29700).

## Appendix A. Supplementary data

Supplementary data associated with this article can be found, in the online version, at doi:10.1016/j.jphotochem.2010.09.001.

## References

[1] D.M. Guldi, G.M.A. Rahman, F. Zerbetto, M. Prato, Carbon nanotubes in electron donor–acceptor nanocomposites, Acc. Chem. Res. 38 (2005) 871–878.
[2] P.J.F. Harris, Carbon nanotube composites, Int. Mater. Rev. 49 (2004) 31–43.
[3] H.G. Chae, T.V. Sreekumar, T. Uchida, S. Kumar, A comparison of reinforcement efficiency of various types of carbon nanotubes in polyacrylonitrile fiber, Polymer 46 (2005) 10925–10935.
[4] H. Miyagawa, M. Misra, A.K. Mohanty, Mechanical properties of carbon nanotubes and their polymer nanocomposites, J. Nanosci. Nanotechnol. 5 (2005) 1593–1615.
[5] M. Baibarac, P. Gomez-Romero, Nanocomposites based on conducting polymers and carbon nanotubes: from fancy materials to functional applications, J. Nanosci. Nanotechnol. 6 (2006) 289–302.
[6] D.M. Guldi, G.M.A. Rahman, N. Jux, D. Balbinot, N. Tagmatarchis, M. Prato, Multiwalled carbon nanotubes in donor–acceptor nanohybrids—towards long-lived electron transfer products, Chem. Commun. (2005) 2038–2040.
[7] M.S. Dresselhaus, G. Dresselhaus, P. Avouris, Carbon Nanotubes: Synthesis, Structure, Properties and Applications, Springer, Berlin, 2001.
[8] S. Reich, C. Thomsen, J. Maultzsch, Carbon Nanotubes: Basic Concepts and Physical Properties, Weinheim, 2004.
[9] B. Shan, K.J. Cho, First principles study of work functions of single wall carbon nanotubes, Phys. Rev. Lett. 94 (2005) 236602–236605.
[10] J.Q. Li, Y.F. Zhang, M.X. Zhang, The electronic structure and its theoretical simulation of carbon nanotube with finited length. Part I. The frontier orbitals and its properties of short armchair nanotubes, Chem. Phys. Lett. 364 (2002) 328–337.

[11] M. Yoshida, J. Aihara, Validity of the weighted HOMO–LUMO energy separation as an index of kinetic stability for fullerenes with up to 120 carbon atoms, Phys. Chem. Chem. Phys. 1 (1999) 227–230.
[12] J. Aihara, H. Kanno, General features of the polyene references graph-theoretically defined for fullerenes, Chem. Phys. Lett. 398 (2004) 440–444.
[13] G.M.A. Rahman, D.M. Guldi, R. Cagnoli, A. Mucci, L. Schenetti, L. Vaccari, M. Prato, Combining single wall carbon nanotubes and photoactive polymers for photoconversion, J. Am. Chem. Soc. 127 (2005) 10051–10057.
[14] E. Kymakis, G.A.J. Amaratunga, Single-wall carbon nanotube/conjugated polymer photovoltaic devices, Appl. Phys. Lett. 80 (2002) 112–114.
[15] E. Kymakis, I. Alexandrou, G.A.J. Amaratunga, High open-circuit voltage photovoltaic devices from carbon–nanotube–polymer composites, J. Appl. Phys. 93 (2003) 1764–1768.
[16] E. Kymakis, G.A.J. Amaratunga, Photovoltaic cells based on dye-sensitisation of single-wall carbon nanotubes in a polymer matrix, Sol. Energy Mater. Sol. Cells 80 (2003) 465–472.
[17] B.J. Landi, R.P. Raffaelle, S.L. Castro, S.G. Bailey, Single-wall carbon nanotube–polymer solar cells, Prog. Photovoltaics 13 (2005) 165–172.
[18] M.Y. Okamura, G. Feher, N. Nelson, in: Govindjee (Ed.), Photosynthesis, New York, 1982.
[19] G. Feher, M.Y. Okamura, The Photosynthetic Bacteria, Plenum, New York, 1978.
[20] K.M. Kadish, K.M. Smith, R. Guilard, The Porphyrin Handbook, Academic Press, New York, 1999.
[21] D.M. Guldi, A. Rahman, V. Sgobba, C. Ehli, Multifunctional molecular carbon materials—from fullerenes to carbon nanotubes, Chem. Soc. Rev. 35 (2006) 471–487.
[22] H. Imahori, Y. Sakata, Fullerenes as novel accepters in photosynthetic electron transfer, Eur. J. Org. Chem. (1999) 2445–2457.
[23] D.M. Guldi, Fullerenes: three dimensional electron acceptor materials, Chem. Commun. (2000) 321–327.
[24] D. Kuciauskas, P.A. Liddell, S. Lin, S.G. Stone, A.L. Moore, T.A. Moore, D. Gust, Photoinduced electron transfer in carotenoporphyrin–fullerene triads: temperature and solvent effects, J. Phys. Chem. B 104 (2000) 4307–4321.
[25] D.M. Guldi, Fullerene–porphyrin architectures; photosynthetic antenna and reaction center models, Chem. Soc. Rev. 31 (2002) 22–36.
[26] T. Vuorinen, K. Kaunisto, N.V. Tkachenko, A. Efimov, H. Lemmetyinen, Photoinduced interlayer electron transfer in alternating porphyrin–fullerene dyad and regioregular poly(3-hexylthiophene) Langmuir–Blodgett films, J. Photochem. Photobiol. A: Chem. 178 (2006) 185–191.
[27] H. Imahori, M. Kimura, K. Hosomizu, S. Fukuzumi, Porphyrin and fullerene-based photovoltaic devices, J. Photochem. Photobiol. A: Chem. 166 (2004) 57–62.
[28] D.M. Guldi, Biomimetic assemblies of carbon nanostructures for photochemical energy conversion, J. Phys. Chem. B 109 (2005) 11432–11441.
[29] P.V. Kamat, Meeting the clean energy demand: nanostructure architectures for solar energy conversion, J. Phys. Chem. C 111 (2007) 2834–2860.
[30] H. Murakami, T. Nomura, N. Nakashima, Noncovalent porphyrin-functionalized single-walled carbon nanotubes in solution and the formation of porphyrin–nanotube nanocomposites, Chem. Phys. Lett. 378 (2003) 481–485.
[31] G.M.A. Rahman, D.M. Guldi, S. Campidelli, M. Prato, Electronically interacting single wall carbon nanotube–porphyrin nanohybrids, J. Mater. Chem. 16 (2006) 62–65.
[32] H.P. Li, B. Zhou, Y. Lin, L.R. Gu, W. Wang, K.A.S. Fernando, S. Kumar, L.F. Allard, Y.P. Sun, Selective interactions of porphyrins with semiconducting single-walled carbon nanotubes, J. Am. Chem. Soc. 126 (2004) 1014–1015.
[33] T. Hasobe, S. Fukuzumi, P.V. Kamat, Ordered assembly of protonated porphyrin driven by single-wall carbon nanotubes: J- and H-aggregates to nanorods, J. Am. Chem. Soc. 127 (2005) 11884–11885.
[34] J. Liu, O. Bibari, P. Mailley, J. Dijon, E. Rouviere, F. Sauter-Starace, P. Caillat, F. Vinet, G. Marchand, Stable non-covalent functionalisation of multi-walled carbon nanotubes by pyrene–polyethylene glycol through π–π stacking, New J. Chem. 33 (2009) 1017–1024.
[35] A. Satake, Y. Miyajima, Y. Kobuke, Porphyrin–carbon nanotube composites formed by noncovalent polymer wrapping, Chem. Mater. 17 (2005) 716–724.
[36] D.M. Guldi, H. Taieb, G.M.A. Rahman, N. Tagmatarchis, M. Prato, Novel photoactive single-walled carbon nanotube–porphyrin polymer wraps: efficient and long-lived intracomplex charge separation, Adv. Mater. 17 (2005) 871–875.
[37] D.M. Guldi, G.N.A. Rahman, J. Ramey, M. Marcaccio, D. Paolucci, F. Paolucci, S.H. Qin, W.T. Ford, D. Balbinot, N. Jux, N. Tagmatarchis, M. Prato, Donor–acceptor nanoensembles of soluble carbon nanotubes, Chem. Commun. (2004) 2034–2035.
[38] D.M. Guldi, G.M.A. Rahman, N. Jux, D. Balbinot, U. Hartnagel, N. Tagmatarchis, M. Prato, Functional single-wall carbon nanotube nanohybrids-associating SWNTs with water-soluble enzyme model systems, J. Am. Chem. Soc. 127 (2005) 9830–9838.
[39] D.M. Guldi, G.M.A. Rahman, M. Prato, N. Jux, S.H. Qin, W. Ford, Single-wall carbon nanotubes as integrative building blocks for solar-energy conversion, Angew. Chem. Int. Ed. 44 (2005) 2015–2018.
[40] D.M. Guldi, G.M.A. Rahman, N. Jux, N. Tagmatarchis, M. Prato, Integrating single-wall carbon nanotubes into donor–acceptor nanohybrids, Angew. Chem. Int. Ed. 43 (2004) 5526–5530.
[41] H.P. Li, R.B. Martin, B.A. Harruff, R.A. Carino, L.F. Allard, Y.P. Sun, Single-walled carbon nanotubes tethered with porphyrins: synthesis and photophysical properties, Adv. Mater. 16 (2004) 896–900.
[42] Z. Guo, F. Du, D.M. Ren, Y.S. Chen, J.Y. Zheng, Z.B. Liu, J.G. Tian, Covalently porphyrin-functionalized single-walled carbon nanotubes: a novel photoactive and optical limiting donor–acceptor nanohybrid, J. Mater. Chem. 16 (2006) 3021–3030.
[43] D.M. Ren, Z. Guo, F. Du, Z.F. Liu, Z.C. Zhou, X.Y. Shi, Y.S. Chen, J.Y. Zheng, A novel soluble Tin(IV) porphyrin modified single-walled carbon nanotube nanohybrid with light harvesting properties, Int. J. Mol. Sci. 9 (2008) 45–55.
[44] D.M. Ren, Z. Guo, F. Du, J.Y. Zheng, Y.S. Chen, Nanohybrid material of SWNTs covalently functionalized with porphyrin for light harvesting antenna: synthesis and photophysical properties, J. Nanosci. Nanotechnol. 7 (2007) 1539–1545.
[45] S. Campidelli, C. Sooambar, E.L. Diz, C. Ehli, D.M. Guldi, M. Prato, Dendrimer-functionalized single-wall carbon nanotubes: synthesis, characterization, and photoinduced electron transfer, J. Am. Chem. Soc. 128 (2006) 12544–12552.
[46] T. Umeyama, M. Fujita, N. Tezuka, N. Kadota, Y. Matano, K. Yoshida, S. Isoda, H. Imahori, Electrophoretic deposition of single-walled carbon nanotubes covalently modified with bulky porphyrins on nanostructured $SnO_2$ electrodes for photoelectrochemical devices, J. Phys. Chem. C 111 (2007) 11484–11493.
[47] A. Osuka, H. Shimidzu, *meso,meso*-linked porphyrin arrays, Angew. Chem. Int. Ed. 36 (1997) 135–137.
[48] A. Tsuda, A. Osuka, Fully conjugated porphyrin tapes with electronic absorption bands that reach into infrared, Science 293 (2001) 79–82.
[49] R.G. Khoury, L. Jaquinod, K.M. Smith, Rational approach to the synthesis of *meso-meso* (5,5′) linked bisporphyrins, Chem. Commun. (1997) 1057–1058.
[50] H. Imahori, K. Tamaki, Y. Araki, Y. Sekiguchi, O. Ito, Y. Sakata, S. Fukuzumi, Stepwise charge separation and charge recombination in ferrocene-*meso,meso*-linked porphyrin dimer–fullerene triad, J. Am. Chem. Soc. 124 (2002) 5165–5174.
Note: The reference is for radical cation of *meso-meso* linked zinc porphyrin dimer.
[51] K. Susumu, T. Shimidzu, K. Tanaka, H. Segawa, Synthesis of novel porphyrin arrays directly-linked through the *meso*-carbons, Tetrahedron Lett. 37 (1996) 8399–8402.
[52] M. Graca, H. Vicente, L. Jaquinod, K.M. Smith, Oligomeric porphyrin arrays, Chem. Commun. (1999) 1771–1782.
[53] M.A. Miller, R.K. Lammi, S. Prathapan, D. Holten, J.S. Lindsey, A tightly coupled linear array of perylene, bis(porphyrin), and phthalocyanine units that functions as a photoinduced energy-transfer cascade, J. Org. Chem. 65 (2000) 6634–6649.
[54] C. Clausen, D.T. Gryko, A.A. Yasseri, J.R. Diers, D.F. Bocian, W.G. Kuhr, J.S. Lindsey, Investigation of tightly coupled porphyrin arrays comprised of identical monomers for multibit information storage, J. Org. Chem. 65 (2000) 7371–7378.
[55] J.L. Bahr, J.M. Tour, Highly functionalized carbon nanotubes using in situ generated diazonium compounds, Chem. Mater. 13 (2001) 3823–3824.
[56] N. Aratani, A. Osuka, Synthesis of *meso-meso* linked hybrid porphyrin arrays by Pd-catalyzed cross-coupling reaction, Org. Lett. 3 (2001) 4213–4216.
[57] L.C. Xu, Z.Y. Li, W. Tan, T.J. He, F.C. Liu, D.M. Chen, Density functional theory studies on the Raman and IR spectra of *meso*-tetraphenylporphyrin diacid, Spectrochim. Acta A 62 (2005) 850–862.
[58] I. Robel, B.A. Bunker, P.V. Kamat, Single-walled carbon nanotube–CdS nanocomposites as light-harvesting assemblies: photoinduced charge-transfer interactions, Adv. Mater. 17 (2005) 2458–2463.
[59] W.H. Zhu, N. Minami, S. Kazaoui, Y. Kim, Fluorescent chromophore functionalized single-wall carbon nanotubes with minimal alteration to their characteristic one-dimensional electronic states, J. Mater. Chem. 13 (2003) 2196–2201.
[60] N. Armaroli, G. Accorsi, J.P. Gisselbrecht, M. Gross, V. Krasnikov, D. Tsamouras, G. Hadziioannou, M.J. Gomez-Escalonilla, F. Langa, J.F. Eckert, J.F. Nierengarten, Photoinduced processes in fullerenopyrrolidine and fullerenopyrazoline derivatives substituted with an oligophenylenevinylene moiety, J. Mater. Chem. 12 (2002) 2077–2087.
[61] C. Trieflinger, H. Rohr, K. Rurack, J. Daub, Multiple switching and photogated electrochemiluminescence expressed by a dihydroazulene/boron dipyrromethene dyad, Angew. Chem. Int. Ed. 44 (2005) 6943–6947.
[62] C. Laurence, P. Nicolet, M.T. Dalati, The empirical treatment of solvent-solute interactions: 15 years of π*, J. Phys. Chem. 98 (1994) 5807–5816.
[63] F. D'Souza, R. Chitta, A.S.D. Sandanayaka, N.K. Subbaiyan, L. D'Souza, Y. Araki, O. Ito, Self-assembled single-walled carbon nanotube: zinc–porphyrin hybrids through ammonium ion-crown ether interaction: construction and electron transfer, Chem. Eur. J. 13 (2007) 8277–8284.
[64] D. Rehm, A. Weller, Kinetics of fluorescence quenching by electron and hydrogen-atom transfer, Isr. J. Chem. 8 (1970) 259–271.
[65] M. Fujitsuka, O. Ito, H. Imahori, K. Yamada, H. Yamada, Y. Sakata, Long-lived charge separation with high quantum yield in a ferrocene–porphyrin–fullerene triad, Chem. Lett. 28 (1999) 721–722.
[66] H. Imahori, H. Yamada, Y. Nishimura, I. Yamazaki, Y. Sakata, Vectorial multistep electron transfer at the gold electrodes modified with self-assembled monolayers of ferrocene–porphyrin–fullerene triads, J. Phys. Chem. B 104 (2000) 2099–2108.
[67] H. Imahori, K. Tamaki, H. Yamada, K. Yamada, Y. Sakata, Y. Nishimura, I. Yamazaki, M. Fujitsuka, O. Ito, Photosynthetic electron transfer using fullerenes as novel acceptors, Carbon 38 (2000) 1599–1605.
[68] C. Luo, D.M. Guldi, H. Imahori, K. Tamaki, K. Sakata, Sequential energy and electron transfer in an artificial reaction center: formation of a long-lived charge-separated state, J. Am. Chem. Soc. 122 (2000) 6535–6551.

[69] K. Yamada, H. Imahori, Y. Nishimura, I. Yamazaki, Y. Sakata, Acceleration of photoinduced charge separation in porphyrin-C-60 dyad with an acetylene spacer, Chem. Lett. 28 (1999) 895–896.
[70] H. Imahori, M.E. El-Khouly, M. Fujitsuka, O. Ito, Y. Sakata, S. Fukuzumi, Solvent dependence of charge separation and charge recombination rates in porphyrin–fullerene dyad, J. Phys. Chem. A 105 (2001) 325–332.
[71] J.M. O'Connell, M.B. Sergei, C.B. Huffman, V.C. Moore, M.S. Strano, E.H. Haroz, K.L. Rialon, P.J. Boul, W.H. Noon, C. Kittrell, J.P. Ma, R.H. Hauge, R.B. Weisman, R.E. Smalley, Band gap fluorescence from individual single-walled carbon nanotubes, Science 297 (2002) 593–596.
[72] L.H. Yu, K. Muthukumaran, I.V. Sazanovich, C. Kirmaier, E. Hindin, J.R. Diers, P.D. Boyle, D.F. Bocian, D. Holten, J.S. Lindsey, Excited-state energy-transfer dynamics in self-assembled triads composed of two porphyrins and an intervening bis(dipyrrinato)metal complex, Inorg. Chem. 42 (2003) 6629–6647.
[73] W.J. Kruper, T.A. Chamberlin, M. Kochanny, Regiospecific aryl nitration of *meso*-substituted tetraarylporphyrins—a simple route to bifunctional porphyrins, J. Org. Chem. 54 (1989) 2753–2756.